Universiti Malaysia Terengganu Journal of Undergraduate Research
Volume 2 Number 3, July 2020: 73-82

eISSN: 2637-1138

THE PERFORMANCE ANALYSIS OF OPTICAL WAVE PROPAGATION FOR UNDERWATER WIRELESS COMMUNICATION

MUHAMMAD SAFIY SABRIL[1,2], FAEZAH JASMAN[2], NURUL ADILAH ABDUL LATIFF[1], SEVIA MAHDALIZA IDRUS[3] AND WAN HAFIZA WAN HASSAN[1*]

[1]*Faculty of Ocean Engineering Technology and Informatics, Universiti Malaysia Terengganu, 21030 Kuala Nerus, Terengganu, Malaysia.*
[2]*Institute of Nano Optoelectronics Research and Technology (INOR), Universiti Sains Malaysia, 11800 USM, Penang, Malaysia.*
[3]*Faculty of Engineering, Universiti Teknologi Malaysia (UTM), 81310 Johor Bahru, Johor, Malaysia.*

**Corresponding author: whafiza@umt.edu.my*

Abstract: Underwater wireless communications refer to transmitting data in an unguided water environment by wireless carriers including acoustic, radio frequency (RF), and optical waves. Relative to acoustic and RF, the optical wave is more promising to offer higher bandwidth at a lower energy consumption rate. However, an optical wave has its challenges such as attenuation due to absorption, scattering and turbulence effects. Therefore, this work attempts to investigate the performance of lightwave propagation for underwater optical wireless communication (UOWC) using simulation and experimental approaches. First, the performance of optical waves was analyzed using MATLAB by simulating the light attenuation model which based on depth-dependent chlorophyll concentration. A depth profile that related to the surface chlorophyll levels for the range 0-4 mg/m3 was used to represent the open ocean. The simulation showed that the attenuation of light less affected for operating wavelength range of 450 – 550 nm. Further, an experimental set-up was developed which consists of a transmitter, receiver, and aquarium to emulate the UOWC channel. Three types of water including clear, sea and cloudy were tested to analyze their interaction with the light emitted by a light-emitting diode (LED) and a laser diode. The emitted light detected by the light sensor and the strength of an audio signal transmitted through the UOWC were measured using a light meter and sound meter respectively. The measured power was plotted against distance and the attenuation constant *c* was deduced through curve fitting method. The analysis showed irrespective of the light sources, UOWC in cloudy water suffered the highest attenuation relative to still clear and seawater. The received power emitted by laser was at least 41% higher than the LED. This study contributes to identify the potential and limitations of different operating schemes to optimize UOWC performance.

Keywords: Underwater optical wireless communication, depth-dependent chlorophyll concentration, optical waves, light attenuation

Introduction

Certainly, surface communication requires a free space channel to transport some information including underwater communications. There are three types of wireless communications used primarily underwater, namely acoustics, radio frequency (RF) and optical communications. The current technology used for communicating underwater is underwater acoustics communication (UWAC) due to the lower power consumption and easier computing complexity for long-distance wireless connections (Kaushal *et al.,* 2016). However, the acoustic wave is restricted in bandwidth and their speed is incredibly low (around 1500 m/s) resulting in serious issues for real-time high-rate communication (Qureshi *et al.,* 2016). On the other hand, underwater optical communication (UWOC) is much higher on bandwidth at lower energy consumption rate, and also lower propagation delay due to the velocity of light is greater than the velocity of sound. Though, studies have shown that optical waves are easily distorted in water, particles and marine microbes, causing the optical scattering that attenuated the optical signals transmitted.

Thus, this work performs an analysis of optical signal propagation in an underwater wireless communication channel environment. The work is divided into two stages including simulation and experimental work. Firstly, the simulation work is carried out using MATLAB software to investigate the light attenuation model based on depth-dependent chlorophyll concentration. Secondly, the experimental work is done to study the behaviour of the received light wave in three types of water (clear, cloudy and seawater – to resemble three types of the ocean water) using LED and laser diode as light sources respectively.

Light Wave Properties

Propagation of optical wave in an underwater environment triggered interaction between each photon and seawater particles which caused the attenuation of the received signal. The attenuation coefficient, $c(\lambda)$, is introduced as a constant measure that summed-up the total energy loss of the transmitted optical signal caused by absorption and scattering processes. Both processes are characterized by absorption coefficient $a(\lambda)$, and scattering coefficient $b(\lambda)$ respectively :

$$c(\lambda) = a(\lambda) + b(\lambda) \quad (1)$$

where $a(\lambda)$ and $b(\lambda)$ are the coefficients that characterize the absorption and scattering processes respectively, and λ is the wavelength of the photon. Absorption is an innumerable process where photons interact with water molecules and other suspended particles and lose their energy thermally while the scattering process losing energy because of the deflection of the photon from the original path. Beer-Lambert's law is used to express the light attenuation effects in UOWC due to its simplicity and commonly used scenario. The received intensity of light is defined as (Zeng *et al.,* 2017)

$$I = I_0 e^{-c(\lambda)d} \quad (2)$$

where I am the intensity of light after the light pass through the media, I_o is the initial light intensity of incident light, c is the attenuation coefficient of the light in media and d is the distance of light travel in media.

The absorption process is grouped into two optical behaviours such as absorption by pure water and absorption by chlorophyll-a. Chlorophyll-a is the primary substance that can be found inside the phytoplankton, photosynthesizing microorganisms and absorption by humic and fulvic acids both are acts as nutrients for phytoplankton (Tahir, 2015). The absorption formula is an addition of these spectra multiplied by their respective concentrations, such that (Johnson *et al.,* 2013):

$$a(\lambda) = a_w(\lambda) + a_f^0 C_f \exp(-k_f \lambda) + a_h^0 C_h \exp(-k_h \lambda) + a_c^0(\lambda)(C_c/C_c^0)^{0.602} \quad (3)$$

where a_w is pure water absorption coefficient in m^{-1}; a^0_f is the specific absorption coefficient of fulvic; a^0_h is the specific absorption coefficient of humic acid; a^0_c is the specific absorption coefficient of chlorophyll in m^{-1}; C_f is the concentration of fulvic acid in mg/m^3; C_h is the concentration of humic acid in mg/m^3; C_c is the concentration of chlorophyll-a in mg/m^3; k_f is the fulvic acid exponential coefficient and k_h is the humic acid exponential coefficient.

The scattering is mainly influenced by two biological factors, scattered by pure water and particulate matter which is characterized as (Johnson *et al.,* 2013):

$$b(\lambda) = b_w(\lambda) + b_s^0(\lambda) C_s + b_l^0(\lambda) C_l \quad (4)$$

where b_w is the pure water scattering coefficient in m^{-1}; b^0_s is the scattering coefficient for small particulate matter in m^2/g; b^0_l is the scattering coefficient for large particulate matter in m^2/g; C_s is the concentration of small particles in g/m^3 and C_l is the concentration of large particles in mg/m^3. The value of these parameters $a(\lambda)$ and $b(\lambda)$ varies with the water type and the wavelength used λ as (Sharifzaedah *et al.,* 2018) and (Pope *et al.,* 1997). However, constant $c(\lambda)$ is only valid for the horizontal link of UOWC and is inaccurate for the vertical link as attenuation is not constant due to marine composition varies significantly with depth (Johnson *et al.,* 2013). Hence, the following subsection presents chlorophyll depth-dependent attenuation model which consider chlorophyll concentration as the variable that varies with the water depth.

Depth Dependent Chlorophyll Attenuation Model

The depth-dependent chlorophyll profiles are used in the chlorophyll-attenuation relationships to determine the depth-dependent attenuation of light. The chlorophyll profile can be modelled as a Gaussian curve which includes five numerically determined parameters, given as (Kameda *et al.,* 1998):

$$C_s(z) = B_0 + Sz + \frac{h}{\sigma\sqrt{2\pi}}\, exp\left[\frac{-(z-z_{max})^2}{2\sigma^2}\right] \quad (5)$$

where $C_c(z)$ is the chlorophyll concentration (mg/m^3) at depth z (m); B_0 is the background chlorophyll concentration at near sea surface (mg/m^3); S is the vertical gradient of chlorophyll concentration (mg/m^3/m); h is the total chlorophyll concentration above the background (mg/m^3); σ is the standard deviation of chlorophyll concentration (m); and z_{max} is the depth of DCM (m). Further, the formula for absorption and scattering from equations (3) and (4) respectively, can be written to include depth-dependency (Johnson *et al.,* 2013):

$$a(\lambda, z) = a_w(\lambda) + a_f^0 \exp(-k_f\lambda)\, C_f(z) + a_h^0 \exp(-k_h\lambda)\, C_h(z) + a_c^0(\lambda, z)[C_c(z)]^{0.602} \quad (6)$$

$$b(\lambda, z) = b_w(\lambda) + b_s^0(\lambda)\, C_s(z) + b_l^0(\lambda)\, C_l(z) \quad (7)$$

where $C_f(z)$, $C_h(z)$ and $C_s(z)$, $C_l(z)$ are the depth-dependent profiles of fulvic and humic acid and small and large particles respectively. These profiles are rewritten by substituting the equation (2.11) into one parameter model introduced by Haltrin that relates the chlorophyll concentration and the concentrations of different particulates (Haltrin, 1999).

Materials and Methods

The methodology for this work is organized into 2 parts namely simulation and experimental work. The following subsection briefly describes each work.

Simulation

The simulation is carried out to mathematically determine the attenuation coefficient of the received light by varying the wavelength of the light sources and the depth of the underwater environment. Nine types of water-based on their varying chlorophyll concentration (S1-S9) are examined to analyse the relationship between the obtained attenuation coefficient with the varying wavelength and depth. The depth-dependent chlorophyll model in (Johnson, 2015) is selected as the attenuation mathematical model in this simulation because, in a real underwater environment, chlorophyll (exist in phytoplankton) are capable of absorbing the transmitted lights. Figure 1 illustrates the simulation workflow to compute the attenuation coefficient based on a depth-dependent chlorophyll model. For simplicity, each step shown in Figure 1 is executed by the self-created MATLAB user-defined function.

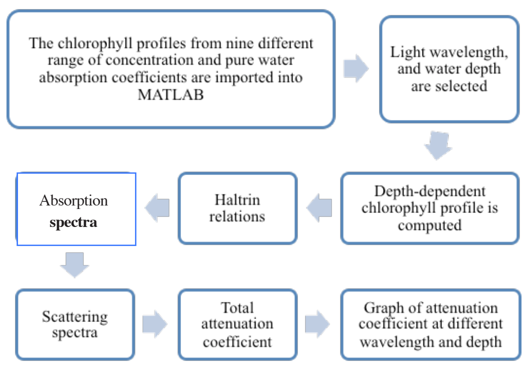

Figure 1: Flow charts for mathematical computation of attenuation coefficient

Experimental Works

The experimental works are divided into two series of experiments. The first experiment is to determine the intensity of the light received in the underwater environment. An aquarium of the dimension 60 cm x 20 cm x 30 cm is used to resemble the underwater environment. Table 1 lists the experimental set-up parameters.

Table 1: Experimental set-up parameters

Components	**Parameters**		
Transmitter/ light source	Aperture diameter (mm)	Wavelength (nm)	Viewing angle (rad)
white LED	8	620 (peak)	2.44
green LED	5	568	0.79
yellow LED	5	587	0.79
red laser	6	650	0.001
Receiver	Aperture diameter (mm)	The spectral range of detection (nm)	
Spherical underwater quantum sensor	61	400-700	

Figure 2 shows the experimental set-up of the first experiment. The light source placed at one end of the aquarium wall acts as the transmitter while the light sensor, LI-COR LI-193R Spherical Underwater Quantum Sensor, is the receiver and the light meter model LI-COR LI-250A is used as the data logger to measure the intensity of the received light.

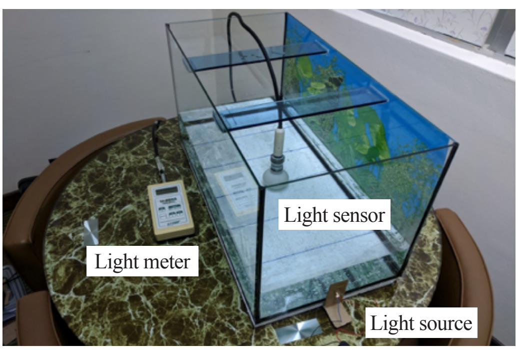

Figure 2: Experiment setup for the first experiment (light intensity)

Further, the second experiment is to measure the strength of sound received when it is transmitted wirelessly underwater. This experiment is conducted as a proof of concept to validate that light can be used as a wireless carrier to bear information (audio) over a short distance. Figure 3 illustrates the set-up for the second experiment. In comparison to the first experiment, the second experiment has an audio signal as the data to be transmitted through the same light sources used in the first experiment. At the receiver end, 0.6 W solar panel is used to convert the light back to the electrical signal and consequently, a speaker is used to convert an electrical audio signal into a corresponding sound. Finally, a decibel meter is used to measure the strength of the received audio signal. In common both experiments are repeated using four types of light sources including white LED, the green LED, yellow LED and red laser. The strength of the received signal is measured at a varying distance of the transmission link from 0 cm up to 50 cm in three types of water: clear, cloudy and seawater. The clear water and seawater are directly collected from the water tap and Batu Rakit Beach respectively while the cold water is the mixture between soda bicarbonate powder with the clear water.

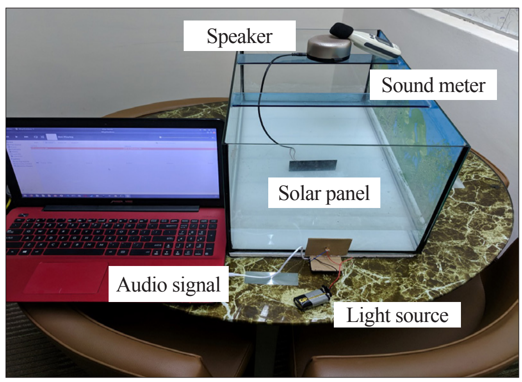

Figure 3: Experiment setup for measuring the second experiment (transmission of the audio signal)

Results and Discussion

Simulation Analysis

The vertical distribution of chlorophyll concentration profiles is categorized into nine groups representing a different range of surface chlorophyll concentrations, namely S1 to S9.

These were <0.04 mg/m^3, 0.04-0.08 mg/m^3, 0.08-0.12 mg/m^3, 0.12-0.2 mg/m^3, 0.2-0.3 mg/m^3, 0.3-0.4 mg/m^3, 0.4-0.8 mg/m^3, 0.8-2.2 mg/m^3 and 2.2-4 mg/m^3, represented by S1-S9 respectively. The full list of the parameter for each of these concentration ranges is given in the (Johnson, 2015). Using these parameters, the chlorophyll profiles for S1-S4 and S5-S6 are plotted in Figure 4 (a) and 4 (b), respectively.

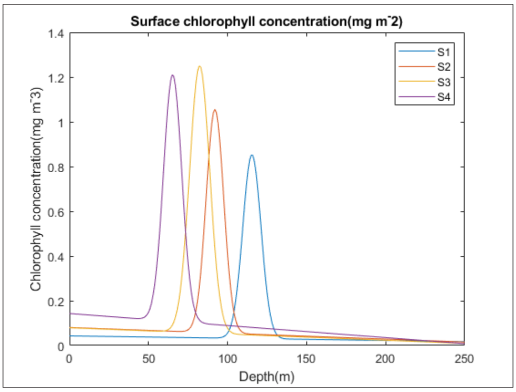

(a)

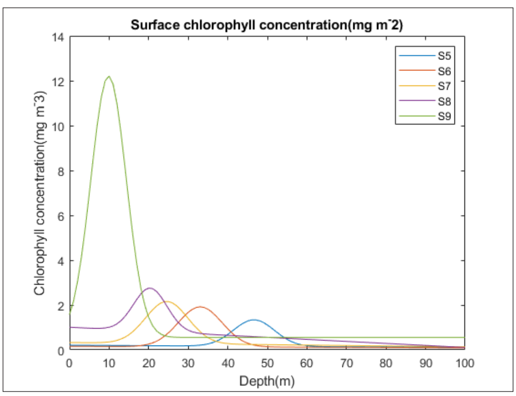

(b)

Figure 4: The depth-dependent chlorophyll profiles for the different range of surface chlorophyll concentration, (a) S1-S4 and (b) S5-S9 respectively

The areas with a low surface chlorophyll concentration, namely S1-S4, the chlorophyll concentration can be up to 0.3 mg/m^3 and the deep chlorophyll maximum (DCM) occurs between 60-120 meters. DCM is a peak in chlorophyll concentration occurs due to an adequate light for photosynthesis and significant nutrient supply at roughly 80m depth (Sigman *et al.,* 2012).

Conversely, areas with a high surface chlorophyll concentration, S5-S9, the DCM occurs near the surface, between 10-40 meters. The high chlorophyll concentration at the surface limits the sunlight to penetrate, thus decreasing the number of phytoplankton and chlorophyll levels in higher depth (Johnson *et al.,* 2013). The chlorophyll profiles in Figure 4 is further utilized to analyze the relationship between the attenuation coefficient and chlorophyll concentration at varying depth and operating wavelength.

As a result, Figure 5 shows three-dimensional plots of attenuation coe-cient variation for the S2 (Figure 5a), and S8 (Figure 5b) profiles at depths between 0 - 250 m for S2 and S4 and 0 - 100 m for S8 and with wavelengths from 400 to 700 nm.

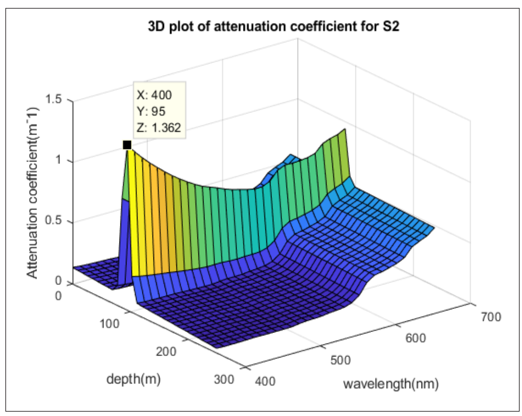

Figure 5(a): The attenuation coefficient varies with the wavelength between 400-700nm and depth between 0-250 meters for S2.

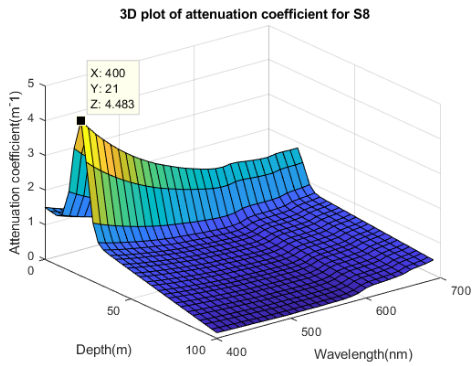

Figure 5(b): The attenuation coefficient varies with the wavelength between 400-700nm and depth between 0-100 meters for S8

Noted that the surface chlorophyll concentrations are 0.04-0.08 mg/m^3 and 0.8-2.2 mg/m^3 for S2 and S8 respectively. The difference between Figure 5(a) and 5(b) is due to the surface chlorophyll concentration and the location of DCM. It is observed that the maximum peak of the attenuation occurs at the depth where the DCM point occurred; i.e., at 95 m and 21 m for S2 and S8 respectively. The optimum operating wavelength for vertical link optical wireless communication configuration in each profile is dependent on the depth of the link, particularly in areas with high surface chlorophyll concentration. For instance, for the S8 profile, the ideal wavelength of a link between 0 to 50 meters is 540 nm, while between 0 to 100 meters this wavelength decreases to 500 nm.

Experiment Analysis

Intensity of Light

Figure 6 shows the normalized received optical power in clear water using four types of light sources. The normalized received power is plotted against the underwater link length from 0 to 50 cm with a gap scale of 10 cm. In common, it is observed that the received power of the optical signal emitted by all the light sources decreased as the underwater link length increased. In comparison to LED light sources, laser diode produced at least 41% higher intensity of received light normalized power. This is most probably because the light beam generated from the laser diode is directional and highly collimated as (Ghassemlooy *et al.,* 2013) and (Shen *et al.,* 2016). The same trend of results is also observed when the sea and cloudy water are used as the UWOC medium.

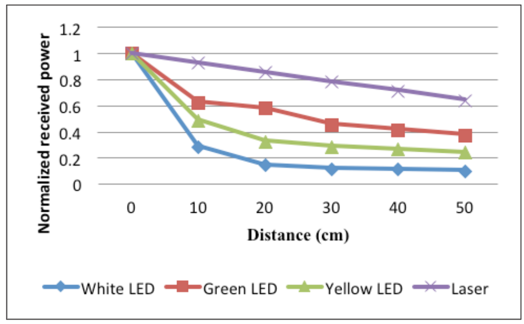

Figure 6: The normalized value of the intensity of a different light source in clearwater

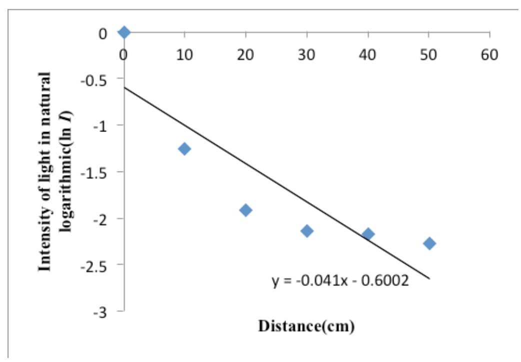

Figure 7: Curve fitting technique to estimate *c* in clear water using white LED as a light source

Figure 7 illustrates the curve fitting method in estimating the attenuation coefficient of the received optical wave from the experiment carried out in this work. The plots in Figure 7 are obtained by applying a natural logarithmic to equation (1) which yields the measured received light in natural logarithmic scale on the vertical axis and deduces the attenuation coefficient from the slope of the curve fitting. It is shown in Figure 12 the estimated *c* in clear water using white LED is 0.041 cm^{-1}.

Table 2: The estimated attenuation coefficient of light intensity from different light sources in 3 types of water

Types of water	Estimated attenuation coefficient (*c*)			
	White LED	Green LED	Yellow LED	Laser
Clearwater	0.041	0.0182	0.0257	0.0088
Cloudy water	0.0683	0.018	0.029	0.0091
Seawater	0.0439	0.02	0.0273	0.0136

Table 2 tabulates the estimated *c* of the received light emitted by all the light sources in three types of water. It is observed that the light emitted from the white LED is heavily attenuated as it obtained the highest estimated *c* compared to other light sources for all types of water. The large viewing angle of white LED (as specified in Table 2) resulted in a bigger received light spot compared to the size of the receiver plane and consequently caused the signal loss. In contrast to the laser where it has a very small viewing angle. Hence, all the transmitted light is fully received by the receiver without any loss. Thus, it justified the minimum estimated *c* (Table 2) obtained by light emitted from laser irrespective of water types.

Comparing the estimated *c* among three types of water, it is apparent the value of *c* in clearwater is the lowest indicating minimum interaction between photon and water particles. In contrast to the estimated *c* in the sea and cloudy water where the light wave is severely attenuated due to frequent interaction photons and other matters. The trend of the obtained results is comparable to the finding in (Kaushal *et al.,* 2016) as the cloudy water encountered the highest estimated *c*. However, it is noted that there are a few estimated *c* in Table 2 against the trend and shall be omitted. These outliers most probably caused by an unforeseen error such as light reflection, and misalignment of transmitter/receiver while conducting the experiments in low light condition.

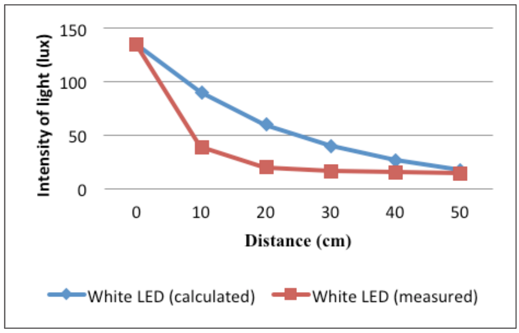

Figure 8: The comparison of measured and calculated values of intensity of the white LED

It is also observed that there is a discrepancy between measured and calculated values at which the light intensity of the calculated values is greater than the measured value. Figure 8 shows the comparison of measured and calculated values of the light intensity emitted by the white LED in clear water. The measured value is lower than the calculated value due to the geometric loss encountered by the received light at the receiver during the experiment. It is observed that the received light spot from the LED source is larger than the receiver area causes the photon to escape from the receiver and leads to energy loss. Therefore, the viewing angle of the light source must be properly aligned to make sure the light beam does not deviate far from the receiver.

Audio Transmission in UOWC

This subsection presents the result obtained from audio transmission in the UOWN experiment. The same analysis as in the first experiment is done. However, due to input power limitation of the light sources, only the light emitted by white LED and laser are capable to carry the audio signal in UOWC. Figure 9 shows the normalized power of the received signal in clear water using white LED and laser light sources respectively. The strength of the audio signal is reducing as the transmission link increases irrespective of the light sources used. Similar to the first experiment, laser light source outperforms white LED particularly when the distance gets farther. This behaviour is also observed in cloudy and seawater environment.

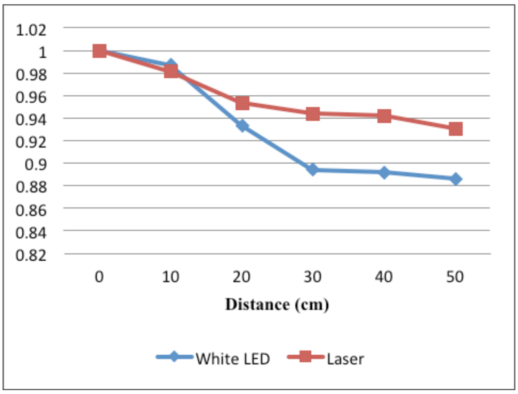

Figure 9: The normalized received power for two light sources in clearwater

Table 3: The attenuation coefficient of the strength of sound of light sources and water types

Types of water	The attenuation coefficient of the strength of sound (cm^{-1})	
	White LED	Laser
Clearwater	0.0027	0.014
Cloudy water	0.0082	0.0061
Seawater	0.0029	0.0032

Further, the estimated attenuation coefficient, *c*, is deduced through curve fitting method as in the first experiment. Table 3 summarizes the estimated *c* for all types of water using white LED and laser respectively. The estimated *c* from the second experiment seemed to be more reliable than the value obtained from the first experiment (Table 2). This is because the values of the estimated *c* for both light sources are increasing accordingly starting from clear, sea and cloudy water following the same trend found in the literature (Kaushal *et al.,* 2016). In common, both experiments validate that laser light source is better than LED but subject to the constraint of higher cost, higher input power and power hazard to eye safety (Ghassemlooy *et al.,* 2013).

Conclusion

This paper presents the performance analysis of the optical wave propagation in UOWC using simulation and experimental approaches. The mathematical simulation of chlorophyll-depth dependent model showed chlorophyll concentration greatly affected the light propagation. The attenuation of the light is maximum when the depth of the light propagates reaches DCM level. Therefore, the right choice of the operating wavelength, location and orientation of the link is essential to minimize the attenuation. The experimental works validate that the received power of lightwave gradually decreases as the transmission link increases due to the attenuation process. The amount of signal degradation is reflected through the estimated attenuation coefficient for each type of water at which the cloudy water is the worst followed by sea and clear water. The high particle concentration in cloudy water makes the light wave hardly to propagate in UOWC environment. Laser light sources perform better than LED because it emits directional and highly collimated light beam but at the price of higher input power, higher cost and power hazard to the eye safety. Thus, a wise selection of system design parameters is crucial to optimize the overall performance.

Acknowledgements

The authors would like to thank the Ministry of Education Malaysia, School of Ocean Engineering, UMT and the administration of UTM for the financial assistance through PDRU fund with vote number 04E58.

References

Bricaud, A., Babin, M., Morel, A., & Claustre, H. (1995). Variability in the chlorophyll-specific absorption coefficients of natural phytoplankton: Analysis and parameterization. *Journal of Geophysical Research*, *100,* 13.

Ghassemlooy, Z., Popoola, W., & Rajbhandari, S. (2013). Optical wireless communications: system and channel modelling with Matlab®. CRC Press.

Haltrin, V. I. (1999). Chlorophyll-based model of seawater optical properties. *Applied Optics*, *38*(33), 6826-6832.

Johnson, L. J., Green, R. J., & Leeson, M. S. (2013). Underwater optical wireless communications: depth dependent variations in attenuation. *Applied Optics*, *52*(33), 7867.

Johnson, L. J. (2015). Optical property variability in the underwater optical wireless channel. University of Warwick, 1-87.

Kameda, T., & Matsumura, S. (1998). Chlorophyll Biomass off Sanriku, Northwestern Pacific, Estimated by Ocean Color and Temperature Scanner (OCTS) and a Vertical Distribution Model. *Journal of Oceanography*, *54*, 509-516.

Kaushal, H., & Kaddoum, G. (2016). Underwater optical wireless communication. *IEEE Access*, *4*, 1518-1547.

Pope, R. M. & Fry, E. S. (1997). Absorption spectrum (380–700 nm) of pure water. ii. integrating cavity measurements. *Applied Optics*, *36*(33), 8710–8723.

Qureshi, U. M., Shaikh, F. K., Aziz, Z., Shah, S. M., Sheikh, A. A., Felemban, E., & Qaisar, S. B. (2016). RF Path and Absorption Loss Estimation for Underwater Wireless Sensor Networks in Different Water Environments. *Sensors (Basel, Switzerland)*, *16*(6), 890. doi:10.3390/s16060890

Shen, C., Guo, Y., Oubei, H. M., Ng, T. K., Liu, G., Park, K. H., Ho, K. T., Alouini, M. S., & Ooi, B. S. (2016). 20-meter underwater wireless optical communication link with 1.5 Gbps data rate. *Optics express, 24*(22), 25502-25509.

Sigman, D. M., & Hain, M. P. (2012). The Biological Productivity of the Ocean: Section 1. *Nature Education Knowledge*, *3*(10).

Sharifzaedah, M., & Ahmadirad, M. (2018). Performance analysis of underwater wireless optical communication systems over a wide range of optical turbulence. *Optics Communications*, *427*, 609-616.

Tahir, F.A. (2015). Open ocean underwater wireless optical communication: chlorophyll and depth dependent variation in attenuation. University Tun Hussein Onn Malaysia, 1-29.

Zeng, Z., Fu, S., Zhang, H., Dong, Y., & Cheng, J. (2017). A survey of underwater optical wireless communications. *IEEE Communications Surveys & Tutorials, 19*(1), 204-238.